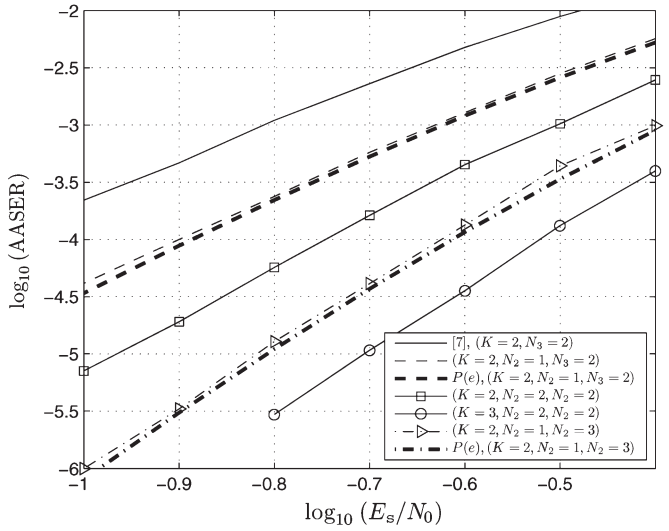

Fig. 6. Asymptotic diversity of ASER for various values of (K, N_2, N_3) with the R_7 relay range scenario.

direct communication between the source and the destination [7], a better AASER can be obtained due to an additional link between the source and the destination. The performance difference is mainly related to the multipath diversity, which is specified by N_2. As any of (K, N_2, N_3) increases, a better ASSER is obtained from an improved diversity gain. In particular, as N_2 increases, a greater performance improvement over the CP-SC system [7] is expected. Fig. 6 shows the ASSER on a log–log plot to verify the diversity gain of the system in the considered SNR values $(4, \ldots, 12)$ dB. Simulated asymptotic diversity gains $G_d = 3.74/4.07/6.2/5.44$ are obtained for $(K = 2, N_2 = 1, N_3 = 2)/(K = 2, N_2 = 2, N_3 = 2)/(K = 3, N_2 = 2, N_3 = 2)/(K = 2, N_2 = 1, N_3 = 3)$. However, in the higher SNR region, diversity gain can be expected to be $G_d \triangleq N_2 + KN_3$.

VII. Conclusion

In this paper, we have proposed an ADF cooperative SC system with multiple relays. Having obtained an ESNR expression, we have derived closed-form expressions for the outage probability and an AASER. In the high-SNR region, the asymptotic outage probability is shown to be the product of all outage probabilities of all links in the system. Multipath diversity between the source and the destination and diversity between the relays and destination are factors in an asymptotic diversity gain. The number of relays affects this diversity as the multiuser diversity gain. This new diversity gain analysis has been verified by simulations.

References

[1] I. E. Telatar, "Capacity of multi-antenna Gaussian channels," *Eur. Trans. Telecommun.*, vol. 10, no. 6, pp. 585–595, Nov./Dec. 1999.

[2] V. Tarokh, H. Jafarkhani, and A. R. Calderbank, "Space–time block codes from orthogonal designs," *IEEE Trans. Inf. Theory*, vol. 45, no. 5, pp. 1456–1467, Jul. 1999.

[3] J. N. Laneman, D. N. C. Tse, and G. W. Wornell, "Cooperative diversity in wireless networks: Efficient protocols and outage behavior," *IEEE Trans. Inf. Theory*, vol. 50, no. 12, pp. 3062–3080, Dec. 2004.

[4] J. N. Laneman and G. W. Wornell, "Energy-efficient antenna sharing and relaying for wireless networks," in *Proc. IEEE Wireless Commun. Netw. Conf.*, Chicago, IL, Oct. 2000, pp. 7–12.

[5] S. Kato, H. Harada, R. Funada, T. Baykas, C. S. Sum, J. Wang, and M. A. Rahman, "Single carrier transmission for multi-gigabit 60-GHz WPAN systems," *IEEE J. Sel. Areas Commun.*, vol. 27, no. 8, pp. 1466–1478, Oct. 2009.

[6] T.-H. Pham, Y.-C. Liang, A. Nallanathan, and H. Garg, "Optimal training sequences for channel estimation in bi-directional relay networks with multiple antennas," *IEEE Trans. Commun.*, vol. 58, no. 2, pp. 474–479, Feb. 2010.

[7] K. J. Kim and T. A. Tsiftsis, "Performance analysis of QRD-based cyclically prefixed single-carrier transmissions with opportunistic scheduling," *IEEE Trans. Veh. Technol.*, vol. 60, no. 1, pp. 328–333, Jan. 2011.

[8] K. J. Kim and T. A. Tsiftsis, "On the performance of cyclic prefix-based single-carrier cooperative diversity systems with best relay selection," *IEEE Trans. Wireless Commun.*, vol. 10, no. 4, pp. 1269–1279, Apr. 2011.

[9] D. Falconer, S. L. Ariyavisitakul, A. B. Seeyar, and B. Edison, "Frequency domain equalization for single-carrier broadband wireless systems," *IEEE Commun. Mag.*, vol. 40, no. 4, pp. 58–66, Apr. 2002.

[10] H. Wicaksana, S. Ting, C. Ho, W. Chin, and Y. Guan, "AF two-path half duplex relaying with inter-relay self interference cancellation: Diversity analysis and its improvement," *IEEE Trans. Wireless Commun.*, vol. 8, no. 9, pp. 4720–4729, Sep. 2009.

[11] Y. Han, S. H. Ting, and A. Pandharipande, "Cooperative spectrum sharing protocol with secondary user selection," *IEEE Trans. Wireless Commun.*, vol. 9, no. 9, pp. 2914–2923, Sep. 2010.

[12] N. C. Beaulieu and J. Hu, "A closed-form expression for the outage probability of decode-and-forward relaying in dissimilar Rayleigh fading channels," *IEEE Commun. Lett.*, vol. 10, no. 12, pp. 813–815, Dec. 2006.

[13] G. K. Karagiannidis, N. C. Sagias, and T. A. Tsiftsis, "Closed-form statistics for the sum of squared Nakagami- m variates and its applications," *IEEE Trans. Commun.*, vol. 54, no. 8, pp. 1353–1359, Aug. 2006.

[14] I. S. Gradshteyn and I. M. Ryzhik, *Table of Integrals, Series, and Products*. New York: Academic, 2007.

[15] B. Devillers, J. Louveaux, and L. Vandendorpe, "About the diversity in cyclic prefixed single-carrier systems," *Elsevier Phys. Commun. J.*, vol. 1, no. 4, pp. 266–276, Dec. 2008.

Deriving Vehicle Speeds From Standard Statistics of Mobile Telecom Switches

Chien-Chun Huang-Fu and Yi-Bing Lin, *Fellow, IEEE*

***Abstract*—Telematics typically utilizes vehicle detectors and Global Positioning System (GPS)-based vehicle probes to compute the speeds of vehicles. When the detectors and the GPS probes are not available, vehicle speeds can be estimated by the cellular floating vehicle data technique, where the telecom network needs to spend extra effort to identify specific users and track their movements. This paper proposes the Speed Determination (SD) Algorithm, which uses standard statistics of telecom switches to compute the speeds of vehicles without extra effort in the telecom network. Simulation and field measurements indicate that the SD Algorithm can effectively report the vehicle speeds of two-way roads.**

***Index Terms*—Little's law, telecom switch, traffic concentration, traffic flow, vehicle speed.**

Manuscript received June 28, 2011; revised September 21, 2011; accepted May 8, 2012. Date of publication June 5, 2012; date of current version September 11, 2012. This work was supported in part by NSC 100-2221-E-009-070, by Chunghwa Telecom, by IBM, by Arcadyan Technology Corporation, by ICL/ITRI, by Nokia Siemens Networks, and by the MoE ATU plan. The review of this paper was coordinated by Dr. F. Bai.

The authors are with the Department of Computer Science, National Chiao Tung University, Hsinchu 300, Taiwan (e-mail: jjfu@cs.nctu.edu.tw; liny@cs.nctu.edu.tw).

Color versions of one or more of the figures in this paper are available online at http://ieeexplore.ieee.org.

Digital Object Identifier 10.1109/TVT.2012.2201968

NOMENCLATURE

The notation used in this paper is listed here.

- d_i Traffic concentration of cell i in a one-way road.
- d_i^* Traffic concentration corresponding to λ_i^*.
- $d_{i,h}$ Heavy traffic concentration corresponding to λ_i.
- $d_{i,l}$ Light traffic concentration corresponding to λ_i.
- D_i Net concentration of both directions in cell i.
- Δt Time interval for statistics.
- f_h Linear equation of the flow–concentration curve for heavy traffic situation; $f_h(\lambda_i) = a_h\lambda_i + b_h$.
- f_l Linear equation of the flow–concentration curve for light traffic situation; $f_l(\lambda_i) = a_l\lambda_i + b_l$.
- λ_i Arrival rate of the users in cell i in a one-way road.
- $\lambda_{1,i}$ Arrival rate of the users in cell i of direction 1 in a two-way road.
- $\lambda_{2,i}$ Arrival rate of the users in cell i of direction 2 in a two-way road.
- λ_i^* Maximum arrival rate of the users in cell i in a one-way road.
- $\mu_{i,j}$ Number of handovers from cell i to cell j.
- μ_i Number of handovers into cell i.
- N_i Number of users in cell i.
- R_i Expected cell residence time that a user stays in cell i.
- ρ_i Voice/data traffic of cell i.
- t_a Intercall arrival time.
- t_c Call-holding time.
- v_i Vehicle speed at cell i.
- x_i Length of cell i.

I. INTRODUCTION

Measuring vehicle speeds and traffic flows on roads is an important issue in telematics. There are three approaches to measuring speed: 1) vehicle detector (VD); 2) Global Positioning System (GPS)-based vehicle probe (GVP) [1], [2]; and 3) cellular floating vehicle data (CFVD) [3]–[5]. By deploying detectors in the roads, the VD approach can accurately measure the speeds of vehicles. However, the deployment and maintenance of the VD approach are expensive. (The detectors must be periodically replaced after their lifetimes.) Both the GVP and the CFVD approaches utilize the mobile telecom network. In the GVP approach, the user equipment in vehicles send the GPS information to the mobile telecom network for speed computation. This approach requires the vehicles to equip with GPS receivers and enable the cellular data transmission all the time. In CFVD, specific users must be identified and tracked by the telecom network to compute their moving speeds on roads. CFVD solutions work well in highway, country, and suburban roads but do not appropriately work in an urban environment. For urban environment, vehicle speeds are typically obtained from the GVP method (where GPS devices are mounted in taxies). Both GVP and CFVD approaches have two major disadvantages: 1) Extra cost (other than normal telecom operation) is required to track a user on the roads, and 2) the privacy of the tracked users must be resolved.

In [6], we derived the expected residence times of users in a specific area through the statistics that can be easily obtained from standard telecom switches. Therefore, we need not modify the existing telecom network or user equipment. In this paper, we extend the aforementioned work to compute the vehicle speed in a road. The idea is described as follows: In a mobile telecom network, the service area is populated with several base stations [BSs, Fig. 1(1)] that are connected to mobile telecom switches called mobile switching centers [MSCs, Fig. 1(2)] or serving GPRS support nodes (SGSNs) [7].

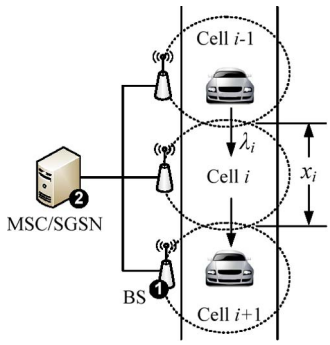

Fig. 1. One-way road covered by cells.

During a phone conversation or Internet data access, the user in a cell (the radio coverage of a BS or a sector of that BS) connects to the MSC/SGSN through the BS. If the user in conversation moves from one cell to another, then the call path is switched from the old cell to the new cell. This process is called *handover*. The MSC/SGSN collects several statistics of the activities for every Δt interval, typically ranging from 15 min to several hours. The recorded statistics include the intercall arrival time t_a, the call holding time t_c, the number $\mu_{i,j}$ of handovers from cell i to cell j, and the *voice/data traffic* ρ_i (in Erlang) of cell i. The traffic measure merits further discussion. For a timeslot Δt, ρ_i is the number of calls arriving at cell i in Δt times the expected call holding time (measured in minutes). In addition, we would like note that the measure of the handover rate is affected by the analysis for overlapping cell regions. Such analysis was implemented in the BS products developed by vendors such as Ericsson, Nokia-Siemens, etc.

From $t_a, t_c, \mu_{i,j}$, and ρ_i, we derived the expected cell residence time R_i that a user stays in cell i as follows [6]: The details are reiterated here for the reader's benefit.

Fact 1: Let μ_i be the number of handovers into cell i in timeslot Δt; that is, $\mu_i = \sum_{j,j\neq i} \mu_{j,i}$. Then, the expected cell residence time R_i can be determined by μ_i and ρ_i as $R_i = \rho_i/\mu_i$.

Proof: Let N_i be the number of users in cell i at timeslot Δt. There are $(\Delta t/t_a)$ call arrivals to a user, which contribute $t_c(\Delta t/t_a)$ call minutes. Therefore

$$\rho_i = \frac{N_i t_c \Delta t}{t_a} \quad \text{or} \quad N_i = \frac{\rho_i t_a}{t_c \Delta t}. \tag{1}$$

Let λ_i be the arrival rate of the users at cell i in timeslot Δt. In Δt, there are $\lambda_i \Delta t$ users moving into cell i. Among these users, (t_c/t_a) of them are in call conversation. In other words, $(\lambda_i \Delta t t_c/t_a)$ users hand over into cell i in Δt, and

$$\mu_i = \frac{\lambda_i \Delta t t_c}{t_a} \quad \text{or} \quad \lambda = \frac{\mu_i t_a}{t_c \Delta t}. \tag{2}$$

Little's Law [6] states that the number N_i of vehicles in a road segment is the vehicle arrival rate λ_i times the traveling time R_i of a vehicle in this road segment; that is

$$N_i = \lambda_i R_i. \tag{3}$$

From (1)–(3), we have

$$R_i = \frac{\rho_i}{\mu_i}. \tag{4}$$

■

In (4), we can use either the arrival (handover-in) rate or the departure (handover-out) rate to compute the response time. The results are about the same in our experiments. In this paper, we will use *Fact 1*

to derive the vehicle speeds in one-way roads and two-way roads. The notation used in this paper is listed in the Appendix.

II. Derivation of the Vehicle Speed

Fig. 1 shows a one-way road covered by cells. In this road, a vehicle (a user) moves from cell $i-1$ to cell $i+1$ through cell i. Let x_i be the length of cell i; then, we have the following result:

Fact 2: The vehicle speed v_i at cell i can be expressed as $v_i = x_i\mu_i/\rho_i$.

Proof: It is clear that the speed v_i is the traveling distance x_i divided by the traveling time R_i or

$$v_i = \frac{x_i}{R_i}. \tag{5}$$

From (4) and (5), we have

$$v_i = \frac{x_i\mu_i}{\rho_i}. \tag{6}$$

■

Note that x_i typically ranges from 500 m to several kilometers and can be obtained through measurement [3], [4]. If a cell covers a two-way road, then it is impossible to directly derive the vehicle speed of each direction from the aforementioned telecom statistics. The major problem is that the ρ_i value is contributed by the vehicles from both directions and cannot be separated to determine the number of vehicles in each direction. We also note that the traffic flow λ_i of each direction provides no hint about the vehicle speeds, as we will elaborate later.

For every one-way road, we can derive a traffic flow–concentration curve that describes the relationship between the traffic flow λ_i and the traffic concentration $d_i = N_i/x_i$, where N_i is the number of vehicles in the road segment of length x_i. Note that the flow–concentration relationship is also affected by other factors, including the lane number of the road, the car-following behavior, etc. The vehicle speed v_i can be expressed by traffic flow and traffic concentration in the following fact:

Fact 3: The vehicle speed v_i at cell i is $v_i = \lambda_i/d_i$.

Proof: We get the proof directly from (3), (5), and the definition $d_i = N_i/x_i$. ■

The traffic flow and the traffic concentration of a road can be obtained from measurement or simulation. A popular simulation tool is VISSIM, which is a microscopic simulation program for multimodal traffic flow modeling [8]. This program accurately simulates urban and highway traffic with various lane numbers. We utilize VISSIM to generate the corresponding flows, concentrations, and vehicle speeds for a three-lane road with Wiedemann 99 car-following model and the Wiedemann Psycho-Physical lane-changing model.

In Table I, v_i, λ_i, and d_i are obtained from the simulation. We compute λ_i/d_i [see Table I(a)] and compare it with v_i [see Table I(b)]. As indicated in Table I(c), the discrepancies are within 1%, which show that *Fact 3* accurately describes the relationship among λ_i, d_i, and v_i.

Based on Table I, Fig. 2 plots the traffic flow–concentration curve. The figure shows that there exists a maximum traffic flow x_i^* that can be accommodated by the road. This figure also indicates that there exists d_i^* such that, if the traffic concentration d_i is smaller than d_i^*, then d_i increases as λ_i increases (light traffic situation). On the other hand, if d_i is larger than d_i^*, then d_i increases as λ_i decreases (heavy traffic situation).

Clearly, a specific $\lambda_i (0 \le \lambda_i \le \lambda_i^*)$ maps to two traffic concentrations $d_{i,l}$ (for light traffic situation) and $d_{i,h}$ (for heavy traffic situation). Both $d_{i,l}$ and $d_{i,h}$ can be approximated by two linear equations, i.e.,

TABLE I
Flows, Concentrations, and Speeds of a Three-Lane Road Example

d_i (veh/km)	13.950	29.982	68.474	113.66	157.24	197.73	270.02	330.59
λ_i (veh/hr)	1170.4	2374.7	4763.4	5380.2	4714.5	4030.7	2817.1	1701.6
λ_i/d_i (km/hr) (a)	83.900	79.204	69.565	47.335	29.982	20.384	10.433	5.147
v_i (km/hr) (b)	83.974	78.646	69.328	47.635	30.028	20.377	10.460	5.173
[(a)-(b)]/(b)	0.089 %	0.710 %	0.341 %	0.629 %	0.153 %	0.035 %	0.255 %	0.502 %

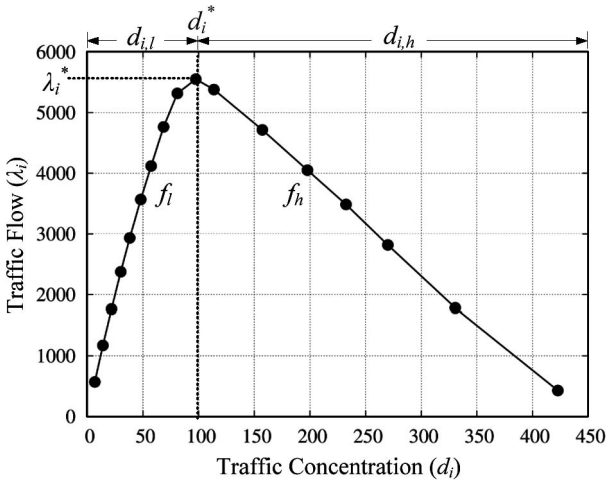

Fig. 2. Traffic flow–concentration curve.

$$d_{i,l} = f_l(\lambda_i) = a_l\lambda_i + b_l \tag{7}$$

$$d_{i,h} = f_h(\lambda_i) = a_h\lambda_i + b_h. \tag{8}$$

Note that, although f_l and f_h may not be exactly linear in the whole range $[0, \lambda_i^*]$, we do observe that, for a specific λ_i, there exist a range $[\lambda_i - \Delta\lambda_i, \lambda_i + \Delta\lambda_i]$ such that the f_l and the f_h segments in this range are linear and can be expressed as the same form as (7) and (8). Now, consider a two-way road where the traffic flows in both directions are $\lambda_{i,1}$ and $\lambda_{i,2}$, respectively. Suppose that the net concentration of both directions is d_i. Then, we have the following fact:

Fact 4: If $a_l \neq a_h$ and $\lambda_{i,1} \neq \lambda_{i,2}$, then the traffic concentrations of both directions can be uniquely determined by $\lambda_{i,1}$, $\lambda_{i,2}$, d_i, (7) and (8).

Proof: From (7) and (8), for traffic flow $\lambda_{i,1}$, the possible traffic concentrations are

$$d_{1,l} = a_l\lambda_{i,l} + b_l \quad \text{and} \quad d_{1,h} = a_h\lambda_{i,1} + b_h.$$

Similarly, for traffic flow $\lambda_{i,2}$, we have

$$d_{2,l} = a_l\lambda_{i,2} + b_l \quad \text{and} \quad d_{2,h} = a_h\lambda_{i,2} + b_h.$$

Now, we prove by contradiction. Let

$$\left.\begin{aligned} D_{l,l} &= d_{1,l} + d_{2,l} \\ D_{l,h} &= d_{1,l} + d_{2,h} \\ D_{h,l} &= d_{1,h} + d_{2,l} \\ D_{h,h} &= d_{1,h} + d_{2,h} \end{aligned}\right\}. \tag{9}$$

It is clear that

$$D_{l,l} < D_{l,h}, D_{h,l} < D_{h,h}. \tag{10}$$

Therefore, if the traffic concentrations cannot be uniquely determined, it means that

$$D_i = D_{l,h} = D_{h,l}. \tag{11}$$

Note that we do not need to consider the combinations $D_{l,l}$ or $D_{h,h}$ due to the relationship (10). From (7), (8), and (11)

$$a_l\lambda_{i,1} + b_l + a_h\lambda_{i,2} + b_h = a_h\lambda_{i,1} + b_h + a_l\lambda_{i,2} + b_l$$

which implies that

$$\mathrm{a}_l(\lambda_{i,1} - \lambda_{i,2}) = \mathrm{a}_h(\lambda_{i,1} - \lambda_{i,2}).$$

Since $\lambda_{i,1} \neq \lambda_{1,2}$, we have $a_l = a_h$, which contradicts the hypothesis. ■

We note that, for a typical road, $a_l \neq a_h$ in the traffic flow–concentration curve, and therefore, the traffic concentrations of both directions can be uniquely determined.

Based on *Fact 4*, the vehicle speeds of both directions of a two-way road can be computed through the following speed determination (SD) algorithm.

SD Algorithm

Step 1: t_a, t_c, $\mu_{i,1}$, $\mu_{i,2}$, and ρ_i from the mobile telecom network for every Δt.

Step 2: Use (1) and (2) to compute $\lambda'_{i,1} = \mu_{i,1}t_a/t_c\Delta t$, $\lambda'_{i,2} = \mu_{i,2}t_a/t_c\Delta t$, and $D'_i = \rho_i t_a/x_i t_c\Delta t$.

Step 3: Plug $\lambda'_{i,1}$ and $\lambda'_{i,2}$ into (7) and (8) to compute $d_{1,l}$, $d_{1,h}$, $d_{2,1}$, and $d_{2,h}$, and obtain $D_{l,l}$, $D_{l,h}$, $D_{h,l}$, and $D_{h,h}$ using (9).

Step 4: For all $a, b \in \{l, h\}$, compute the errors for $d_{a,b}$, where

$$\mathrm{Error}[D_{a,b}] = \frac{|D_{a,b} - D'_i|}{D'_i}.$$

Step 5: For $x, y \in \{l, h\}$, if

$$\mathrm{Error}[D_{x,y}] = \min_{a,b\in\{l,h\}} (\mathrm{Error}[D_{a,b}])$$

then the speeds for directions 1 and 2 are $v_{1,x}$ and $v_{2,y}$, respectively.

In the next section, we show that the SD Algorithm can accurately select the speed of each direction in a two-way road.

III. Numerical Examples

In this section, we extend the VISSIM simulation to accommodate voice/data call activities. We simulate the 6-km segment of a two-way road of three lanes in each direction. In each simulation round, up to 36 000 vehicles are injected in the road during six simulated hours. To avoid initial effect, we only observe the behavior of the vehicles after two simulated hours. The desired speed of a vehicle is uniformly randomly selected between 60–120 km/h (for light traffic situation) and 5–60 km/h (for heavy traffic situation). The road is covered by six cells (where a cell coverage is 1 km). In this simulation, $t_a =$ 60 min, $\Delta t = 15$ min, and t_c ranges from 1 to 30 min, which simulates the behavior of MSC/SGSN that collects $\mu_{i,1}$, $\mu_{i,2}$, and ρ_i for every Δt. We first validate Step 2 of the SD Algorithm by comparing the measured $\lambda_{i,1}$, $\lambda_{i,2}$, and D_i with $\lambda'_{i,1}$, $\lambda'_{i,2}$, and D'_i. Note that we can consider a Δt shorter than 15 min by resetting the range parameter at the cost of sending more messages from the telecom switches to the application database. However, with a short Δt, the obtained vehicle speed information may be too dynamic yet nonstable to be useful. Therefore, $\Delta t = 15$ min is selected.

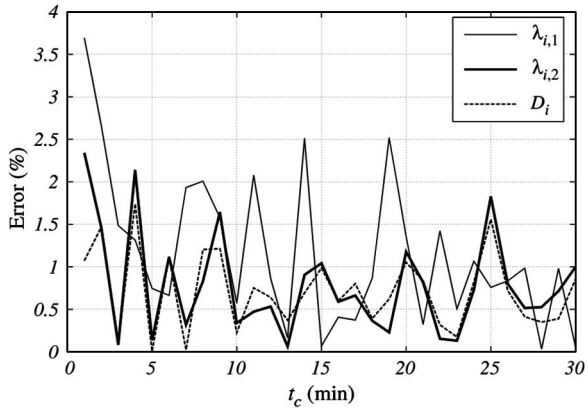

Fig. 3. Errors between the measured data and (1) and (2) computed in Step 2 of the SD Algorithm ($t_a = 60$ min, $\Delta t = 15$ min, $\lambda_{i,1} =$ 2374.7 veh/h, $\lambda_{i,2} = 2817.1$ veh/h, and $D_i = 300.004$ veh/km).

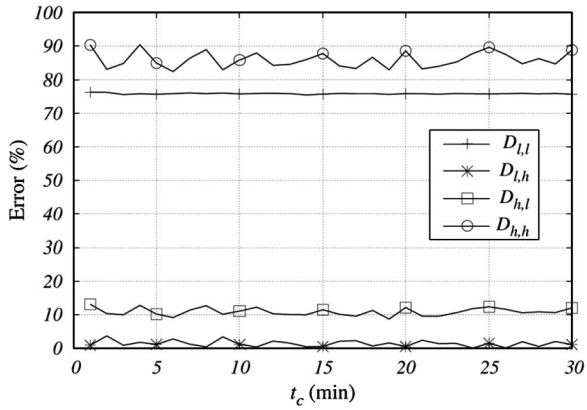

Fig. 4. Errors between $D_{a,b}$ and $D_i\prime$ ($t_a = 60$ min, $\Delta t = 15$ min, $\lambda_{i,1} =$ 2374.7 veh/h, $\lambda_{i,2} = 2817.1$ veh/h, and $D_i = 300.004$ veh/km).

Fig. 3 plots the errors $\mathrm{Error}[\lambda'_{i,1}] = |\lambda'_{i,1} - \lambda_{i,1}|/\lambda_{i,1}$, $\mathrm{Error}[\lambda'_{i,2}] = |\lambda'_{i,2} - \lambda_{i,2}|/\lambda_{i,2}$, and $\mathrm{Error}[D'_i] = |D'_i - D_i|/D_i$ against t_c, where the direction-1 flow is $\lambda_{i,1} = 2374.7$ veh/h and $d_{i,1} = 29.982$ veh/km (light traffic situation), and the direction-2 flow is $\lambda_{i,2} = 2817.1$ veh/h and $d_{i,2} = 270.022$ veh/km (heavy traffic situation). In this case, $D_i = d_{i,1} + d_{i,2} = 300.004$ veh/km. The figure indicates that the errors between the measured data and (1) and (2) computed by the SD Algorithm are smaller than 4% and, in most cases, smaller than 1.5%.

Fig. 4 shows that, in the example of Fig. 3, the SD Algorithm correctly selects the traffic concentration (and, therefore, the vehicle speed) of each direction for various t_c values. By using the $\mu_{i,1}$, $\mu_{i,2}$, and ρ_i collected from the simulation, we compute $D_{l,l}$, $D_{l,h}$, $D_{h,l}$, and $D_{h,h}$ (Step 3 of the SD Algorithm) and obtain the errors between them and D'_i (Step 4 of the SD Algorithm). For various t_c values, the SD Algorithm always finds the correct traffic concentration (which is $D_{l,h}$), and the vehicle speeds for both directions are $v_{1,l} =$ 78.646 km/hr and $v_{2,h} = 10.460$ km/hr, respectively.

Fig. 5 shows that the SD Algorithm correctly selects the concentration for various flow combinations where $t_a = 60$ min, $t_c = 1$ min, and $\Delta t = 15$ min. In this figure, we consider $\lambda_{i,1} = 2374.7$ veh/h with light traffic, and $\lambda_{i,2}$ ranges from 1500 to 5500 veh/h with heavy traffic. In Fig. 5, the concentration selected is $D_{l,h}$, which indicates that the SD Algorithm always correctly selects the concentrations. Same results are observed for other flow combinations and are not presented.

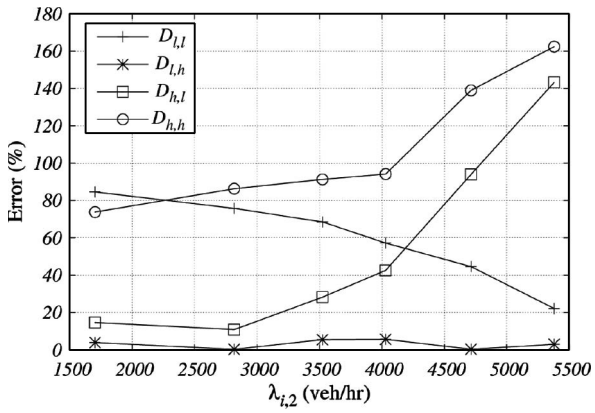

Fig. 5. Errors between $D_{a,b}$ and D'_i ($t_a = 60$ min, $t_c = 1$ min and $\Delta t = 15$ min, $\lambda_{i,1} = 2374.7$ veh/h, $d_{i,1} = 29.982$ veh/km, $\lambda_{i,2}$: heavy traffic, and 113.66 veh/km $< d_{i,2} <$ 330.61 veh/km).

Fig. 6. Measuring the traffic data from real road.

We have obtained the traffic flows and vehicle speeds of a road at Taoyuan, Taiwan, on November 11, 2010 (see Fig. 6). The speeds and traffic flow data for this road segment were published by the Ministry of Transportation and Communications (MOTC), Taiwan, which were measured by the VD at the 66 km of the road [9]. We have also obtained μ_i and ρ_i from the mobile telecom network from a cell of length $x_i = 1.5$ km and $\Delta t = 60$ min, where the BS is located at 66.8 km of the road.

Based on *Fact 2*, we derived the vehicle speeds from μ_i and ρ_i at 14, 15, 18, and 19 hours of the day and compare them with the VD data reported by MOTC, Taiwan. The errors between (6) and the VD data range from 3.74% to 11.36% (see Table II). Since the traffic flows and the speeds measured from the VD are about the same for both directions of the road, our method results in the same speeds for both directions.

IV. Conclusion

This paper has proposed an SD Algorithm that uses standard statistics of telecom switches to compute the speeds of vehicles without extra computation or message delivery efforts in telecom network. Our study indicated that the SD algorithm can reasonably capture the vehicle speeds with 3%–12% errors, compared with the field data reported by MOTC, Taiwan. These errors are partly caused by noise and variation in the footprint of areas covered by the cell towers (and other factors described here). In Table II, the noise became serious at hour 18 in the observation period. To further reduce the errors by eliminating these factors is a great challenge and will be our top-priority for future work. As compared with other approaches, the SD algorithm is reasonably accurate. For example, in [3], errors of 10% for intercity freeway and 24%–32% for urban freeway were reported.

TABLE II
Errors Between Our Method and the Vehicle Detector

Time (hour)	ρ_i (min)	μ_i (per hr)	Speed (km/hr)		Error
			Eq. (6)	VD66	
14	111.65	144.5	116.480	107.875	7.98%
15	112.50	130	104.000	108.042	3.74%
18	124.40	128.5	92.966	104.875	11.36%
19	85.97	106	110.973	104.292	6.41%

Our study also introduces several interesting issues for future research: A major factor contributing to the inaccuracy of the SD algorithm (as well as GVP and CFVD approaches) is that the investigated cell covers an area larger than the road, where the statistics of the telecom switches also include activities of users not in the road (e.g., noncar users). Such call activity "noise" may reduce the accuracy of the estimated speeds. In our study, the cell selected is a sector of UMTS BS with the directional antenna pointing along the road, which significantly reduces the possibility of involving the users not in the road.

Another issue is that vehicles exiting from and entering to the freeway also contribute to the average speeds. It may be desirable to separately derive the speeds of exiting and nonexiting vehicles.

As a final remark, this work is pending U.S., Taiwan, and China patents.

References

[1] J.-C. Herrera, D.-B. Work, R. Herring, X. Ban, Q. Jacobson, and A.-M. Bayen, "Evaluation of traffic data obtained via GPS-enabled mobile phones: The mobile century field experiment," *Transp. Res. C, Emerging Technol.*, vol. 18, no. 4, pp. 568–583, Aug. 2010.

[2] P. Chakroborty and P. Kikuchi, "Using bus travel time data to estimate travel times on urban corridors," *Transp. Res. Rec.*, vol. 1870, pp. 18–25, 2004.

[3] H. Bar-Gera, "Evaluation of a cellular phone-based system for measurements of traffic speeds and travel times: A case study from Israel," *Transp. Res. C, Emerging Technol.*, vol. 15, no. 6, pp. 380–391, Dec. 2007.

[4] D. Gundlegard and J.-M. Karlsson, "Handover location accuracy for travel time estimation in GSM and UMTS," *IET Intell. Transp. Syst.*, vol. 3, no. 1, pp. 87–94, Mar. 2009.

[5] J. Ygnace, "Travel time/speed estimates on the French Rhone corridor network using cellular phones as probes," SERTI V Progr., Lyon, France, 2001, Final Rep.

[6] Y.-B. Lin, M.-F. Chang, and C.-C. Huang-Fu, "Derivation of cell residence times from the counters of mobile telecom switches," *IEEE Trans. Wireless Commun.*, vol. 10, no. 12, pp. 4048–4051, Dec. 2011.

[7] Y.-B. Lin and A.-C. Pang, *Wireless and Mobile All-IP Networks*. Chichester, U.K.: Wiley, 2005, 528 p.

[8] *VISSIM 5.10 User Manual*, Planung Transport Verkehr AG, Karlsruhe, Germany.

[9] Ministry of Transportation and Communications. [Online]. Available: http://www.motc.gov.tw/